AUTOMATIC LEVELLING OF A PLATFORM TO ACHIEVE ARTIFICIAL GRAVITY

Carlos M. N. Velosa[1] , Levin Gerdes[2] , Martin Zwick[3]

[1] PTP for the European Space Agency (ESA/ESTEC), 2201 AZ Noordwijk, The Netherlands, E-mail: carlos.velosa@esa.int

[2] GTP for the European Space Agency (ESA/ESTEC), 2201 AZ Noordwijk, The Netherlands, E-mail: levin.gerdes@esa.int

[3] HE Space for the European Space Agency (ESA/ESTEC), 2201 AZ Noordwijk, The Netherlands, E-mail: martin.zwick@esa.int

ABSTRACT

This paper presents a control algorithm for the automatic levelling of a platform intended to emulate artificial microgravity on ground. The platform is supported in three points, the inclination of the platform is obtained via a high accuracy inclinometer and the levelling is performed with three high precision linear stepper motors. The algorithm is implemented in a microcomputer showing the experimental validation that the platform is successfully levelled around the specified orientation. By slightly tilting the platform one can introduce very small lateral forces that serve to simulate microgravity.

Keywords: Air Bearings, Microgravity, Levelling Platform, ROOTLESS.

1 INTRODUCTION

The use of air bearings to simulate microgravity on Earth is a technique that has been used since the beginning of spaceflight [1]. Conventional air bearing platforms resort to compressed air to create a thin layer with a few tens of microns between two surfaces, minimizing the friction between the bodies. This way, a given platform, for example with air bearings on the bottom surface of the platform and facing down, can float freely on a flat floor/surface.

The European Space Agency (ESA) developed in-house a new concept to simulate microgravity in two dimensions resorting to a holonomic robot that presents several advantages when compared to conventional air bearing platforms [2], [3].

The robotic platform, named ROOTLESS (Robotic Testbed for Floating-Dynamics Simulation), is based on a holonomic robot that can move in any direction from any initial pose at any given moment.

When compared to conventional air bearing platforms this platform allows experiments with fewer restrictions in terms of time and space. The working space is limited only by the length of the hose supplying compressed air to the air bearings facing upwards and supporting the plate with the payload.

Moreover, the platform allows the simulation of microgravity in 2D at a very low cost, as opposed to the conventional air bearing platforms. Building and maintaining an extremely flat floor/surface for experiments is expensive and can be impractical for instance for universities and small research institutes.

One of the drawbacks of the robotic platform is related to the mecanum wheels that allow the movement of the robot in any direction. The point of contact between the wheels and the floor is not continuous because of the gap between each roller of the wheel. Moreover, as the wheel rotates the rollers collide with the floor and this effect introduces substantial vibrations in the vertical direction that perturbs the payload.

A separated structure including a spring-damper system was built between the robot and the levelling platform to minimize the undesirable vertical vibrations. Such a solution reduced indeed the vertical vibrations but it demonstrated not to be enough to promptly compensate the irregularities of the floor.

That is why an active control system is required to level automatically the platform/floating plane. This way, the system can auto-calibrate the height of the air bearings on an irregular floor and can also introduce an artificial gravity by slightly tilting the horizontal floating plane.

Fig.1 shows the mobile robot with the levelling platform:

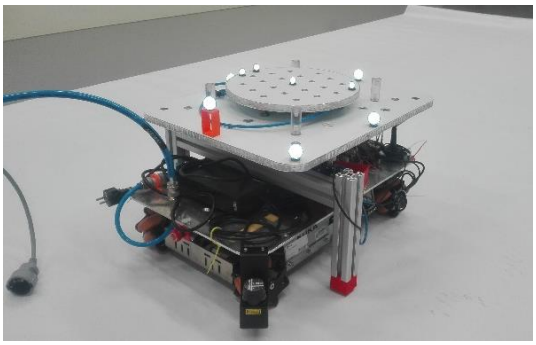

Figure 1: ROOTLESS with the levelling platform.

Besides this particular application, the potential applications for automatic levelling systems, either for military or for civil purposes, are numerous. An automatic landing surface to allow helicopters to land on ships travelling in rough seas, artillery/missiles launcher platforms, vehicle-borne radar systems, focus-tuning in semiconductor manufacturing and medical nursing beds are merely examples of that.

There is a number of automatic levelling systems presented in the literature, relying most of them in three, four or six supporting points/legs to level the platform [4]–[9]. However, very few works can be found regarding the automatic levelling of a platform capable of supressing undesirable high frequency and low amplitude vibrations.

The present work presents an algorithm to level with high precision a given platform supported on three points.

The paper is organized as follows: the problem to be solved is stated in section 2; section 3 presents the solution to the problem; in section 4 the results of the experimental validation are presented; and section 5 concludes the paper.

2 PROBLEM STATEMENT

Consider a rectangular platform supported on three points and three linear stepper motors each one placed at one of the three points. Fig.2 shows the disposition of the motors on the platform: two motors in the front; and one motor in the back. The designation FL, FR and B stands for Front Left motor, Front Right motor and Back motor, respectively.

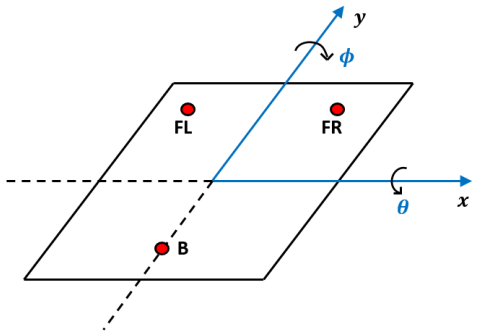

Figure 2: Disposition of the motors on the platform.

The purpose of the work is to find a control solution that levels automatically the platform around the specified angles θ_{ref} and ϕ_{ref}. For that, an inclinometer provides the rotation around the x axis (pitch angle - θ) and around the y axis (roll angle - ϕ) and it is and placed in the centre of the platform. Given that one of the objectives of the levelling platform is to achieve artificial microgravity by tilting the platform around one of the directions (very small angles), the inclinometer considered is of high resolution ($\delta = 0.0002778°$) and with a range of $\pm 1°$. The inclinometer is analog and its output voltage is $\pm 5V$, corresponding to $\pm 1°$. The linear stepper motors are bipolar motors, operating at $12V$, and are also of high precision, with a linear travel step of $\kappa = 1.5$ µm.

3 APPROACH PROPOSED

The control is divided into two parts: the control of the roll motion, ϕ; and the control of the pitch motion, θ, and it is based on flowcharts. For the control of the roll motion, ϕ, the FL and FR motors are placed initially in the middle positions (between the lowest positions and the highest positions) and then the roll angle, ϕ, is measured. If the platform is tilted in the positive direction of the y axis (clockwise direction), the control algorithm increases successively the step of the FR motor and decreases the step of the FL motor until the platform is levelled. On the other hand, if the platform is tilted in the negative direction of the y axis (anticlockwise direction), the control algorithm decreases successively the step of the FR motor and increases the step of the FL motor until the platform is levelled again. This way the platform is levelled around the reference/desired angle, $\phi_{ref} - \delta < \phi < \phi_{ref} + \delta$. δ denotes the resolution of the inclinometer. The entire algorithm is described in Fig.3:

Control of the Roll Angle, ϕ:

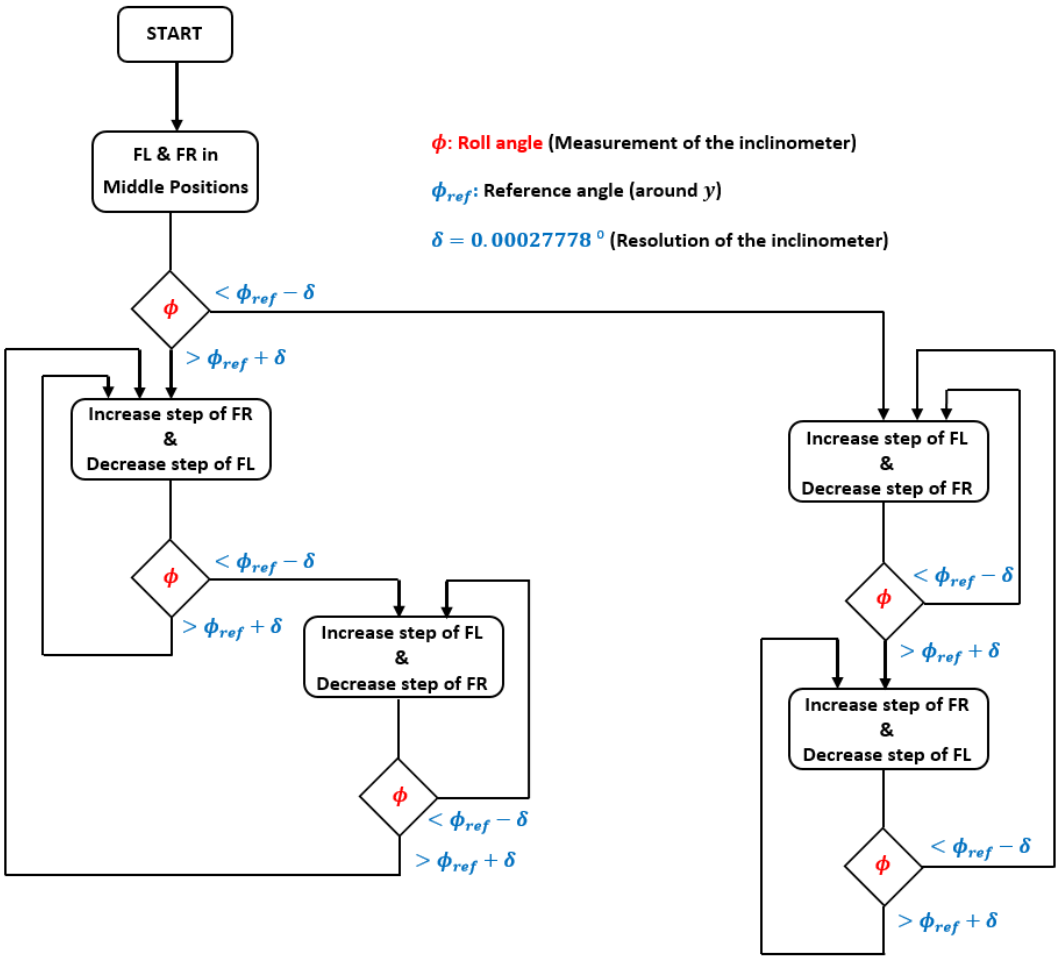

Figure 3: Flowchart of the control of the roll angle, ϕ.

The control of the pitch angle, θ, is achieved similarly to the control of the roll angle, ϕ. The FL, FR and B motors are placed initially in the middle positions and then the motors go up or down (increasing or decreasing the steps) depending on which direction the platform is tilted around the x axis.

The motors have a normally open switch that closes when the motors are in the lowest positions. These switches are used as inputs to the microcomputer to indicate that the motors are in known positions. This way, all the motors are placed initially in the lowest positions, because this is the way to know where they are, and then they are increased by fixed number of steps (determined experimentally) to achieve the middle positions.

The entire algorithm is described in Fig.4:

Control of the Pitch Angle, θ:

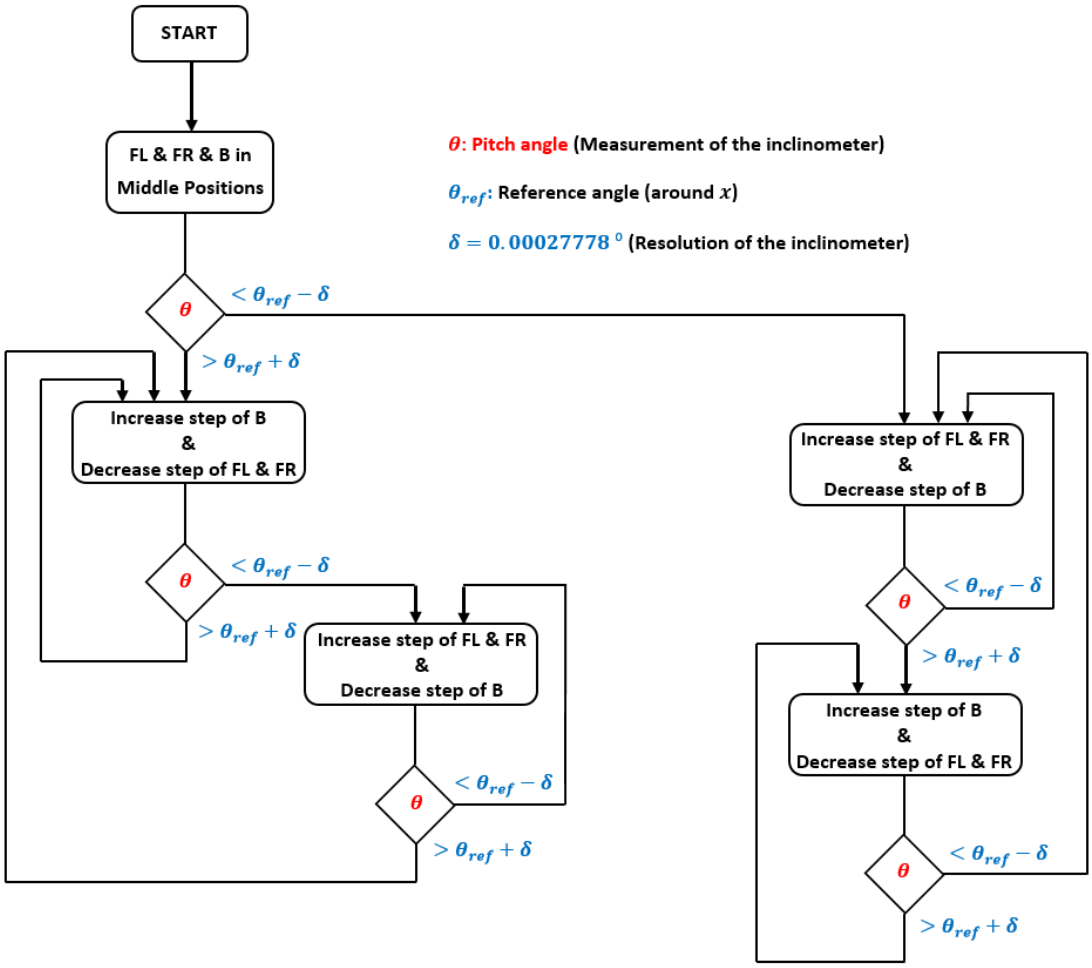

Figure 4: Flowchart of the control of the pitch angle, θ.

4 EXPERIMENTAL VALIDATION

The control algorithm was implemented on a BeagleBone Black (BBB) microcomputer in C++. The data from the inclinometer is analog ($\pm 5V$), and in order to read that data with the BBB, a 16-bit Analog-to-Digital Converter (ADC) was used in between. The communication between the ADC and the BBB is done via Serial Peripheral Interface (SPI). The three step motors are controlled by digital signals from the BBB and these signals are connected to the motor drivers. Fig.5 shows the block diagram of the controller:

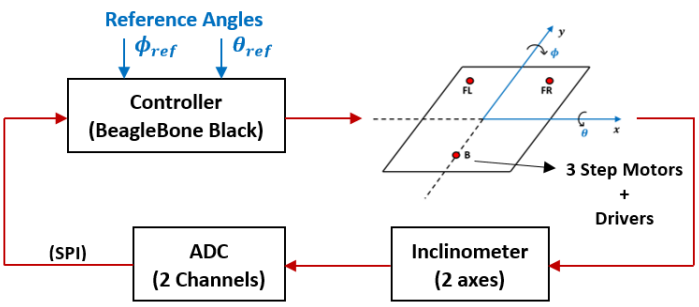

Figure 5: Block diagram of the controller.

Due to the physical limitations of the stepper motors, that is, how fast the motors can move, the pulse width of the control signals sent to the motors was set in 3 μs and the time between consecutive pulses in 1 μs. These values were determined experimentally. For lower values, the motors experienced jitter (noise and vibration without any motion).

The time between successive readings of the inclinometer (the time given by the program to perform the analog to digital conversion in the ADC) was set in 10 μs. The control signals are sent to the motors immediately after each measurement of the inclinometer. This means that the steps of the motors are increased/decreased at a frequency of $f = 1/((3+1+10)\times 10^{-6}) = 71.4$ kHz. In other words, a linear travel step of $\kappa = 1.5$ μm is achieved every 14 μs. Taking into account the distance between the control points B and $\overline{\text{FL. FR}}$, $d = 35$ cm, this corresponds to an angle of $\theta = \arcsin((1.5\times 10^{-6})/0.35) = 0.2456\times 10^{-3}$ °.

Note that the inclination with respect to a single step of the motor is inferior to the resolution of the inclinometer, $\delta = 0.2778\times 10^{-3}$ °. This means that at least two steps have to be performed in order to measure the respective difference.

If one considers the maximum range of the inclinometer, 1°, takes into account the distance between the control points B and $\overline{\text{FL. FR}}$, $d = 35$ cm, and the fact that the motors can move simultaneously, that is, one motor going up and the other going down at the same time, the maximum angle can be achieved in 28.5 ms.

Before the actual control starts, all the motors go to the middle positions, which are located at 1 cm above the lowest positions. This corresponds to a waiting time of 9.3 s. However, this time is not problematic at all because the experiments with the payload start only after this initial period.

In short, one has that an angle of $0.2456\times 10^{-3}\times 2 = 0.4912\times 10^{-3}$ ° (two motors, one going up and the other going down) can be achieved every 14 μs, which demonstrates to be fast enough to compensate the irregularities of an uneven floor.

By tilting the platform, small lateral forces are transmitted to the payload and microgravity is achieved. Here is an example of Phobos (one of the moons of Mars), where an inclination of the platform of $\alpha = 0.0333$ ° is required to achieve a gravity of $g = 0.0057$ m/s^2. Another example is the asteroid 21-Lutetia, where an inclination of $\alpha = 0.2920$ ° is required for a gravity of $g = 0.05$ m/s^2.

Considering the resolution of the inclinometer, $\alpha = \delta = 0.2778\times 10^{-3}$ °, the minimum artificial gravity that can be emulated is $g = 9.81\sin(0.2778\times 10^{-3}) = 4.756\times 10^{-5}$ m/s^2. Taking into account the maximum angle provided by the inclinometer around each axis, $\alpha = 1$°, the maximum artificial gravity that can be achieved is $g = 9.81\sin(1) = 0.1712$ m/s^2.

In what follows some results to show the capability of the robot tracking the platform are presented. The experiment is divided into two tests. In the first test, the platform is levelled around $(\phi,\theta) = (0,0)$° and a very small force is initially applied to the platform (where the payload is installed) in the x direction. This way, the robot follows the platform primarily in the x direction. In reality the robot tracks the platform in both directions, x and y, but the largest position variation is in the x direction. The absolute position of the robot and of the platform is provided by a Vicon system installed in the facility. In the second test, the platform is slightly tilted around the positive direction of y, and the platform moves in the x direction due to the introduced artificial gravity. Figs.6-9 show the results. Fig.6 represents the position of the platform and of the robot in the x and y directions for the case of zero gravity. Fig.7 represents the respective relative positions of the platform with respect to the robot. Fig.8 represents the positions of the objects for the case of artificial gravity, and Fig.9 the respective relative positions.

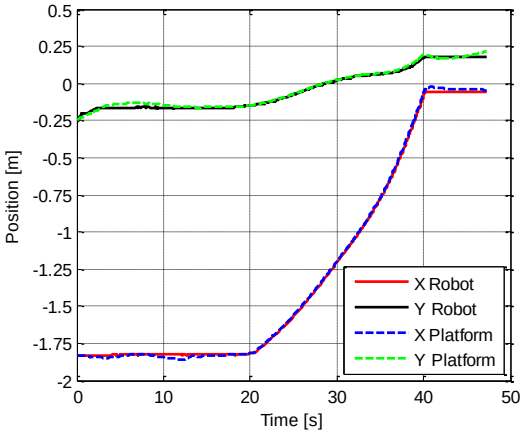

Figure 6: Positions of the platform and of the robot (zero gravity).

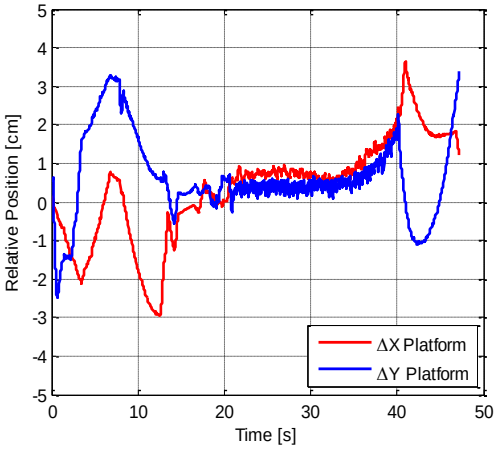

Figure 7: Relative positions of the platform with respect to the robot (zero gravity).

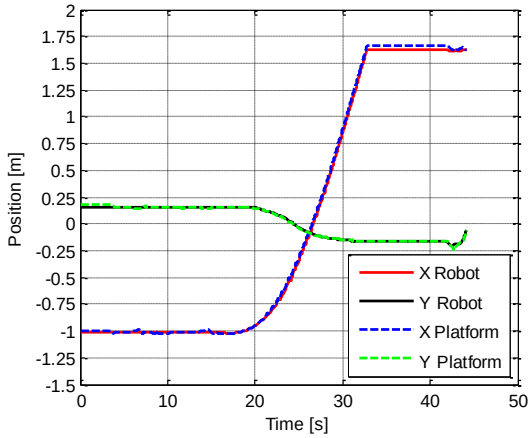

Figure 8: Positions of the platform and of the robot (artificial gravity).

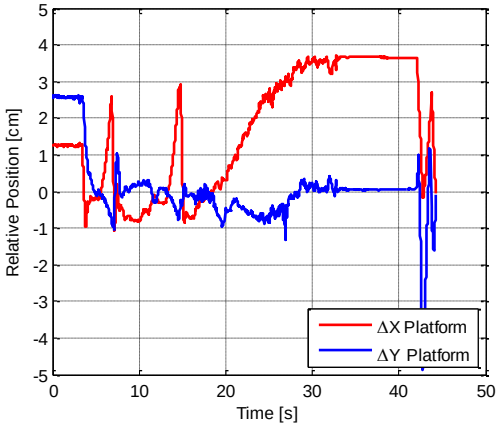

Figure 9: Relative positions of the platform with respect to the robot (artificial gravity).

Note that for the case of zero gravity the variation of the position of the platform in the x direction, which occurs approximately between 20 and 40 s, is supposed to be linear, see Fig.6. In reality this variation is linear at least between 20 and 30 s. Between 30 and 40 s a small acceleration is observed but this acceleration is introduced by the robot due to the ability of the robot to track the payload (performance of the tracking controller).

In comparison to the case of artificial gravity, see Fig.8, the position of the platform in the x direction varies clearly according to a parabolic curve, between approximately 17 and 25 s, indicating that the platform moves with a positive acceleration along this direction. Between 25 and 33 s it occurs that the position varies linearly because the maximum velocity of the robot, $V = 0.8\,\mathrm{m/s}$, is achieved (movement with constant velocity and zero acceleration). The constant segments before and after these variations correspond to the periods where the robot was manually stopped.

Analysing the relative position of the platform with respect to the robot, see Fig.7, the plot can be interpreted in three parts: the first period, between 0 and 20 s, corresponds to the period where the robot is manually stopped and the platform moves freely (air bearings ON); the second period, between 20 and 40 s, where the robot tracks the platform with a given offset; and the third period, after 40 s, where the robot is manually stopped and the platform continues the motion. To prevent the platform from moving away from the air bearings some end stops were installed on the levelling platform. This explains why the platform reaches a maximum in the x direction and then goes back, see Δx, – the platform reaches the end stop.

Analysing Fig.9, the plot can be interpreted in four segments: the first period, between 0 and 4 s, corresponding to the period where the air bearings are OFF and the platform does not move; the period between 4 and 17 s, where the position of the platform was adjusted by an operator; the period between 17 and 42 s, where the robot tracks the platform; and the period after 42 s where the platform was moved again by the operator. In this particular case, the offset of the platform in the x direction increases with time and the platform reaches the end stop at $t = 30$ s, only 2 s before the robot is manually stopped.

Note that in both tests there is also the residual acceleration due to the resolution of the inclinometer. In practice, the orientation $(\phi, \theta) = (0,0)°$ cannot be achieved. One has that $-\delta < \phi, \theta < \delta$, corresponding to the residual acceleration of $g = 4.756 \times 10^{-5}\ \mathrm{m/s^2}$.

5 CONCLUSION

An algorithm to control a levelling platform supported on three points has been presented in this paper. The algorithm is based on a flowchart and allows the stabilization of the platform around the specified angles with high precision, allowing consequently the simulation of artificial microgravity. Given the nature of the algorithm, the error of the stabilized platform is very small and it is only given by the resolution of the inclinometer. The algorithm is easy to implement and requires neither a mathematical model of the system nor extensive tuning of the parameters of the controller.

As a future work it would be interesting to modify the control algorithm in such a way that one can have a given attraction point in the centre of a circle attracting the payload while the robot moves along that circle. This would allow for example the simulation of microgravity of a body orbiting an asteroid, a comet or a small moon.

Acknowledgement

This work was conducted in the Automation & Robotics Section of the European Space Research

and Technology Centre of the European Space Agency (ESA/ESTEC) in Noordwijk, the Netherlands, and supported by the Portuguese Foundation for Science and Technology (FCT) and by the German Aerospace Center (DLR) through the following programs:

References

[1] J. Schwartz, M. Peck, and C. Hall, "Historical Review of Air-Bearing Spacecraft Simulators," *J. Guid. Control. Dyn.*, vol. 26, no. 4, pp. 513–522, 2003.

[2] H. Kolvenbach and K. Wormnes, "Recent Developments on ORBIT, a 3-DOF Free Floating Contact Dynamics Testbed," in *13th International Symposium on Artificial Intelligence, Robotics and Automation in Space (i-SAIRAS 2016)*, 2016, pp. 1–7.

[3] H. Kolvenbach and K. Wormnes, "A Robotic Testbed For Low-Gravity Simulation," in *13th International Symposium on Artificial Intelligence, Robotics and Automation in Space (i-SAIRAS 2016)*, 2016, pp. 1–7.

[4] H. Yang, "A Mechatronic Levelling System Based on Parallel Manipulator," in *2010 2nd International Conference on Industrial Mechatronics and Automation (ICIMA)*, 2010, pp. 248–251.

[5] H. Yang, "Research on Dynamics of a Three-DOF Parallel Manipulator for Levelling Mechanism," *Adv. Mater. Res.*, vol. 774–776, pp. 1369–1374, 2013.

[6] X. Gang and S. Chai, "Optimal load balancing leveling method for multi-leg flexible platforms," *Chinese J. Mech. Eng.*, vol. 26, no. 5, pp. 900–908, 2013.

[7] Y.-P. Wang and S.-C. Tien, "A Model-Based Iterative Approach for the Parallelism and Gap Control of Two Platforms," *Trans. Inst. Meas. Control*, vol. 36, no. 5, pp. 654–661, 2014.

[8] S. A. Conyers, N. I. Vitzilaios, M. J. Rutherford, and K. P. Valavanis, "A Mobile Self-Leveling Landing Platform for VTOL UAVs," in *2015 IEEE International Conference on Robotics and Automation (ICRA)*, 2015, pp. 815–822.

[9] Z. Qiliang, S. Jianghong, and H. Shifeng, "Control Strategy of Three-Point Supported Automatic Levelling Platform," in *2015 IEEE 12th International Conference on Electronic Measurement & Instruments*, 2015, pp. 693–697.